A pulsated weak-resonant-cavity laser diode with transient wavelength scanning and tracking for injection-locked RZ transmission

Gong-Ru Lin,[1,*] Yu-Chieh Chi,[1] Yu-Sheng Liao,[1,2] Hao-Chung Kuo,[2] Zhi-Wang Liao,[3] Hai-Lin Wang,[3] and Gong-Cheng Lin[3]

[1]*Graduate Institute of Photonics and Optoelectronics, Department of Electrical Engineering, National Taiwan University, No.1, Sec. 4, Roosevelt Road, Taipei 106, Taiwan*
[2]*Department of Photonics & Institute of Electro-Optical Engineering, National Chiao Tung University, 1001 Ta Hsueh Road, Hsinchu 300, Taiwan*
[3]*Telecommunication Laboratories Advanced Technology, Chunghwa Telecom Co., Ltd., Taoyuan, Taiwan*
**grlin@ntu.edu.tw*

Abstract: By spectrally slicing a single longitudinal-mode from a master weak-resonant-cavity Fabry-Perot laser diode with transient wavelength scanning and tracking functions, the broadened self-injection-locking of a slave weak-resonant-cavity Fabry-Perot laser diode is demonstrated to achieve bi-directional transmission in a 200-GHz array-waveguide-grating channelized dense-wavelength-division-multiplexing passive optical network system. Both the down- and up-stream slave weak-resonant-cavity Fabry-Perot laser diodes are non-return-to-zero modulated below threshold and coherently injection-locked to deliver the pulsed carrier for 25-km bi-directional 2.5 Gbits/s return-to-zero transmission. The master weak-resonant-cavity Fabry-Perot laser diode is gain-switched at near threshold condition and delivers an optical coherent pulse-train with its mode linewidth broadened from 0.2 to 0.8 nm by transient wavelength scanning, which facilitates the broadband injection-locking of the slave weak-resonant-cavity Fabry-Perot laser diodes with a threshold current reducing by 10 mA. Such a transient wavelength scanning induced spectral broadening greatly releases the limitation on wavelength injection-locking range required for the slave weak-resonant-cavity Fabry-Perot laser diode. The theoretical modeling and numerical simulation on the wavelength scanning and tracking effects of the master and slave weak-resonant-cavity Fabry-Perot laser diodes are performed. The receiving power sensitivity for back-to-back transmission at bit-error-rate $<10^{-10}$ is –25.6 dBm, and the power penalty added after 25-km transmission is less than 2 dB for all 16 channels.

OCIS codes: (140.3520) Lasers, injection-locked; (060.2330) Fiber optics communications.

References and links

1. S. J. Park, C. H. Lee, K. T. Jeong, H. J. Park, J. G. Ahn, and K. H. Song, "Fiber to the home services based on wavelength division multiplexing passive optical network," J. Lightwave Technol. **22**(11), 2582–2591 (2004).
2. K. Lee, J. H. Song, H. K. Lee, and W. V. Sorin, "Multistage access network for bidirectional DWDM transmission using ASE-injected FP-LD," IEEE Photon. Technol. Lett. **18**(6), 761–763 (2006).
3. W. Lee, M.-Y. Park, S.-H. Cho, J. Lee, C. Kim, G. Jeong, and B.-W. Kim, "Bidirectional WDM-PON based on gain-saturated reflective semiconductor optical amplifiers," IEEE Photon. Technol. Lett. **17**(11), 2460–2462 (2005).
4. S. C. Lin, S. L. Lee, and C. K. Liu, "Simple approach for bidirectional performance enhancement on WDM-PONs with directmodulation lasers and RSOAs," Opt. Express **16**(6), 3636–3643 (2008).

#163683 - $15.00 USD Received 1 Mar 2012; revised 9 May 2012; accepted 12 May 2012; published 4 Jun 2012

5. J. Prat, C. Arellano, V. Polo, and C. Bock, "Optical network unit based on a bidirectional reflective semiconductor optical amplifier for fiber-to-the-home networks," IEEE Photon. Technol. Lett. **17**(1), 250–252 (2005).
6. G.-R. Lin, T.-K. Cheng, Y.-C. Chi, G.-C. Lin, H.-L. Wang, and Y.-H. Lin, "200-GHz and 50-GHz AWG channelized linewidth dependent transmission of weak-resonant-cavity FPLD injection-locked by spectrally sliced ASE," Opt. Express **17**(20), 17739–17746 (2009).
7. K.-M. Choi, J.-S. Baik, and C.-H. Lee, "Broad-band light source using mutually injected Fabry-Pérot laser diodes for WDM-PON," IEEE Photon. Technol. Lett. **17**(12), 2529–2531 (2005).
8. Q. T. Nguyen, P. Besnard, L. Bramerie, A. Shen, C. Kazmierski, P. Chanlou, G.-H. Duan, and J.-C. Simon, "Bidirectional 2.5-Gb/s WDM-PON using FP-LDs wavelength-locked by a multiple-wavelength seeding source based on a mode-locked laser," IEEE Photon. Technol. Lett. **22**(11), 733–735 (2010).
9. Z. Xu, Y.-J. Wen, W.-D. Zhong, C.-J. Chae, X.-F. Cheng, Y. Wang, C. Lu, and J. Shankar, "High-speed WDM-PON using CW injection-locked Fabry-Pérot laser diodes," Opt. Express **15**(6), 2953–2962 (2007).
10. S. Sivaprakasam and R. Singh, "Gain change and threshold reduction of diode laser by injection-locking," Opt. Commun. **151**(4-6), 253–256 (1998).
11. Y.-C. Chang, Y.-H. Lin, J. H. Chen, and G.-R. Lin, "All-optical NRZ-to-PRZ format transformer with an injection-locked Fabry-Pérot laser diode at unlasing condition," Opt. Express **12**(19), 4449–4456 (2004).
12. L. Li, "Static and dynamic properties of injection-locked semiconductor lasers," IEEE J. Quantum Electron. **30**(8), 1701–1708 (1994).
13. C. C. Lin, Y. C. Chi, H. C. Kuo, P. C. Peng, C. J. Chang-Hasnain, and G.-R. Lin, "Beyond-bandwidth electrical-pulse modulation of a TO-can packaged VCSEL for 10 Gbit/s injection-locked NRZ-to-RZ transmission," J. Lightwave Technol. **29**(6), 830–841 (2011).
14. Y.-C. Chang, Y. H. Lin, J. H. Chen, and G.-R. Lin, "All-optical NRZ-to-PRZ format transformer with an injection-locked Fabry-Pérot laser diode at unlasing condition," Opt. Express **12**(19), 4449–4456 (2004).
15. E.-K. Lau, L.-J. Wong, and M.-C. Wu, "Enhanced Modulation Characteristics of Optical Injection-Locked Lasers: A Tutorial," IEEE J. Sel. Top. Quantum Electron. **15**(3), 618–633 (2009).
16. P. P. Vasil'ev, *Ultrafast Diode Lasers: Fundamentals and Applications* (Artech House, 1995), Chap. 3.

1. Introduction

Developing the dense-wavelength-division-multiplexing passive optical networks (DWDM-PONs) with narrower channel spacing and/or a higher channel data rate is the mainstream research for global high-speed communication toward large channel capacity and multi-access services [1]. Versatile DWDM-PON architectures with acceptable capacity and flexibility have emerged as candidates for subscriber networks to meet the demand of the next-generation fiber-to-the-home applications. With filtered amplified spontaneous emission (ASE) injection-locking of Fabry-Perot laser diodes (FPLDs) [2], reflective semiconductor optical amplifiers (RSOAs) [3–5], or weak-resonant-cavity Fabry-Perot laser diodes (WRC-FPLDs) [6], several types of quasi-color-free transmitters were considered to overcome the DWDM-channelized mode-selection problem that occurred on conventional single-mode laser diode transmitters. However, spectrally sliced incoherent ASE suffers from a large-intensity noise to limit the bit rate below 2.5 Gbit/s for these injection-locking transmitters. Alternatively, coherent injection-locking schemes using new master broad-band light sources (BLSs) such as mutually injection-locked FPLD [7] and a quantum-dash passively mode-locked laser (QD-MLL) [8] have been proposed recently. Mutually injected antireflection-coated FPLDs have been employed to injection-lock slave FPLDs for 100-Mbit/s transmission with 100 GHz channel spacing [7]. Later on, a highly coherent continuous-wave (CW) light injection-locked FPLD based 10-Gbit/s bi directional DWDM-PON architecture was reported [9]. Nevertheless, all these coherence-injection applications require a precise control on the wavelength of the master and the slave lasers, such that the shortcomings on wavelength maintenance and stability are accompanied for practical DWDM-PON systems.

The proposed approaches currently remain limited by the colorless ASE spectrum, low operating bandwidth, high power budget, and high intensity-noise when applied to a practical DWDM-PON link. Despite these drawbacks, the concept of a coherent master ASE injection-locked slave laser diode has become oriented as a new solution toward high-bit-rate DWDM-PONs. Moreover, the return-to-zero (RZ) carrier with a sufficiently short duty-cycle has been successfully used in optical time division multiplexing (OTDM) networks for on-off-keying (OOK) data transmission. Combining the DWDM and OTDM techniques in future fiber-optic

#163683 - $15.00 USD Received 1 Mar 2012; revised 9 May 2012; accepted 12 May 2012; published 4 Jun 2012

networks is considered at the current stage for enabling the maximum usage of spectral and temporal channel capacities in both systems. This paper, demonstrates a novel pulsated WRC-FPLD source with transient wavelength scanning and tracking effects. Such a unique master laser with dense longitudinal modes is used as the partially coherent BLS in the DWDM-PON system to concurrently solve the problems of non-coherence and small injection-locking range accompanied with conventional injection-locked transmitters. The concept of this work is emphasized on the injection-locked RZ carrier generation and data transmission using the master and slave WRC-FPLDs under pulsated operation. Specifically, the master WRC-FPLD exhibits a transiently wavelength self-scanning capability to facilitate the wavelength self-tracking and locking with the slave WRC-FPLD. Through coherent injection-locking with the spectrally sliced and pulsated master WRC-FPLD, the directly non-return-to-zero (NRZ) modulated slave WRC-FPLD successfully delivers a pulsed RZ data stream for bi-directional DWDM-PON transmission at 2.5 Gbit/s. Without using any data-format converter, the wavelength scanning of the pulsated master WRC-FPLD mode simultaneously triggers both the coherent injection-locking and the NRZ-to-RZ transformation in slave WRC-FPLDs. Such an operation is free from the wavelength presetting or monitoring circuitry because the pulsed WRC-FPLD can provide wavelength self-scanning and self-tracking functions to injection-lock the slave WRC-FPLD automatically. Specifically, the transient wavelength scanning and tracking effect of the master and slave WRC-FPLDs are theoretically modeled and numerically simulated, which explains the broadened mode spectrum of the master WRC-FPLD pulse for enlarging the injection-locking range of the slave WRC-FPLD. After 200-GHz array waveguide grating (AWG) channelization, this study analyzes both the back-to-back and 25-km transmission performances of the bidirectional WRC-FPLD RZ transmitter at 2.5 Gbit/s.

2. Experimental setup

The proposed bidirectional 2.5 Gbit/s RZ DWDM-PON is quasi-color-free with the entire slave WRC-FPLDs coherently injection-locked by the pulsating master WRC-FPLD, as shown in Fig. 1. The WRC-FPLD is generally a buried hetero-structure FPLD with different end-face reflectances. First, the WRC-FPLD was fabricated by growing an n-type InP layer with a thickness of 200 nm and a dopant concentration of 5 x 10^{18} cm^{-3} on a substrate. Two 200-nm-thick cladding n-type InP films were employed with the same dopant concentration of N = 2 × 10^{18} cm^{-3}. The active InGaAsP layer consists of 0.9% compressively strained multi-quantum wells with a thickness of 50 Å at an emission wavelength of 1.55 μm, and the 0.6% tensile-strained layers with a thickness of 85 Å at a bandgap wavelength of 1.1 μm were employed as the barrier. The temperature-dependent wavelength shift of such a WRC-FPLD effectively decreases with a $\Delta\lambda/\Delta T$ slope of lower than 0.08 nm/°C, which is close to the typical value for common quantum-well-based FPLDs. Thereafter, the upper cladding layers including a 5000-Å-thick intrinsic InP followed by two p-type InP layers with a corresponding thickness of 100 nm/1.2 μm and doping concentrations of 1 × 10^{17} / 1 × 10^{18} cm^{-3}, respectively, were grown on the gain region. Finally, a p-type InGaAs layer with a thickness and dopant concentration of 200 nm and 2 × 10^{18} cm^{-3}, respectively, was deposited as the top contact layer. The master WRC-FPLD with an integrated optical isolator was gain switched for injection-locking the down- and up-stream slave WRC-FPLDs. The master WRC-FPLD was gain switched at a near-threshold condition and exhibited a relative intensity noise (RIN) of −130 dBc/Hz. The output pulse-train of the master WRC-FPLD was amplified by an Erbium-doped fiber amplifier (EDFA) and channelized by a 200-GHz AWG to function as the multi-wavelength coherent seeding source. The longitudinal-mode wavelength of the master WRC-FPLD was temperature detuned to match one of the DWDM channels. Down- and up-stream slave WRC-FPLD injection-locking was performed by the C-band beam splitter/combiner (BS/BC). The WRC-FPLD is generally a conventional buried heterostructure FPLD with specific end-face reflectance.

#163683 - $15.00 USD Received 1 Mar 2012; revised 9 May 2012; accepted 12 May 2012; published 4 Jun 2012

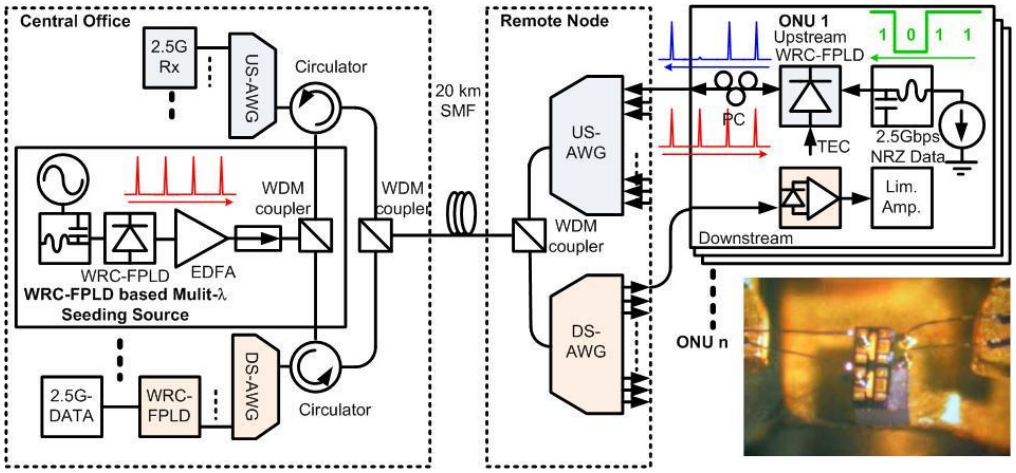

Fig. 1. Bi-directional quasi-color-free WRC-FPLD-based 2.5-Gbit/s RZ DWDM-PON with a pulsed coherent injection locker. Lower right inset: the bird's-eye view magnified image of the WRC-FPLD packed in a TO-can mount with bonding wires linked to the cathode and anode pins of the mount.

Free-running, such a WRC-FPLD, shows a threshold current (up to 27 mA) that is substantially larger than that of a conventional FPLD (approximately 10 mA), as shown in Fig. 2(a). The resonant cavity length of all WRC-FPLDs was 300 μm with a corresponding longitudinal mode spacing of 1.2 nm. The back and front facet reflectances of these WRC-FPLDs were 94% and 1%, respectively. Such a highly asymmetric coating design allows efficient external injection from the front facet to reduce the power budget and the high reflectance at the rear facet of the WRC-FPLD to reduce the power consumption. This is a trade-off set by the end-facet reflectance of the WRC-FPLD under injection-locking case. The reduced reflectivity of the facet allows an efficient external injection into the WRC-FPLD; however, the WRC-FPLD cavity cannot hold most of the external injection after round-trip circulation in the WRC-FPLD. That is, the injection power level must be increased because the higher free running power is also dissipated from this facet with low reflection, in comparison with a facet with normal reflectance. Fiber pigtailing for the transistor outline can (TO-56-can)-packed WRC-FPLD is also supported by the laser diode manufacturer using laser fusing–splicing technology. For reducing the surface reflectance, the end-face of a single-mode fiber (Corning, SMF28) was polished to an 8° angle with respect to its surface normal. After injection-locking by the master WRC-FPLD, the WRC-FPLD was directly modulated by a 2.5 Gbit/s pseudorandom binary sequence (PRBS) data stream with a pattern length of 2^{23}-1 for transmission performance diagnosis. The V_{p-p} of the electrical PRBS data is set as 1 V (from 0 to 1 V). The NRZ data were encoded directly on the WRC-FPLD by reducing its bias current to below the threshold condition, which displays a nonlinear relationship with the external injection power or photon density [10–12]. All of the bit-error-rate (BER) data were taken using a commercial receiver (Sanway Optoelectronics tech. Corp. Ltd, SI1525-80ATOS-S) in connection with an error detector (Hewlett Packard, 70842B). Prior to BER analysis, the temperature of the WRC-FPLD varied from 20°C to 40°C to adjust the number of injection-locked modes involved within a single AWG-channelized spectral window. An increase in injection-locked modes within one DWDM channel, signifies a highly coherent optical carrier obtained for transmission at a lower BER.

3. Results and discussions

The phenomenon of threshold current reduction for a laser diode under external injection-locking has been comprehensively investigated [10,11]. Nevertheless, such a technique is

#163683 - $15.00 USD Received 1 Mar 2012; revised 9 May 2012; accepted 12 May 2012; published 4 Jun 2012

usually limited by insufficient power injected into a laser diode with relatively high end-face reflectance. To reduce the threshold current of a commercial FPLD by 2 mA, the external injection power must be amplified to overcome the transmission loss caused by high end-face reflectance of FPLD. In contrast, the power-current characteristics of the slave WRC-FPLD at different injection levels are shown in Fig. 2(a), and it reduces the threshold current by 10 mA as the external injection power increases up to 9 dBm. The inset of Fig. 2(a) shows that such a high threshold current caused by 1% front-facet reflectance of the WRC-FPLD resonant cavity can be suppressed by considerably 30% or more. External injection compensates the loss of the resonant cavity, facilitating the lasing of the WRC-FPLD to build up at lower driving currents. The threshold current reduction can be theoretically derived as [13,14]

$$\Delta I_{th} = \frac{qV}{\tau_c}\left(\frac{2\kappa}{g}\frac{1}{\sqrt{1+\alpha^2}}\sqrt{\frac{S_{inj}}{S_0}}\right), \tag{1}$$

where q denotes the electronic charge, V the volume of the active region, τ_c the carrier lifetime in active region, κ the coupling coefficient, g the stimulated emission rate, α the linewidth enhancement factor, S_{inj} the photon number injected into the WRC-FPLD cavity, and S_0 the steady-state photon number [12–14]. The power-current slope remains almost constant at injection powers ranging between −12 and + 3 dBm. In this case, the reshaping on rising and falling edges of the generated RZ data at different injection levels can be negligible if the DC bias point of the WRC-FPLD is up-shifted to a higher level. The external quantum efficiency, which is linearly proportional to the power-current slope of the WRC-FPLD, is not degraded with an enlarged injection, as shown in Fig. 2(a). The RZ data-stream generation from a slave WRC-FPLD directly modulated by a PRBS NRZ data stream is shown in Fig. 2(b), which is initiated under external injection by a pulse-train from the master gain-switched WRC-FPLD.

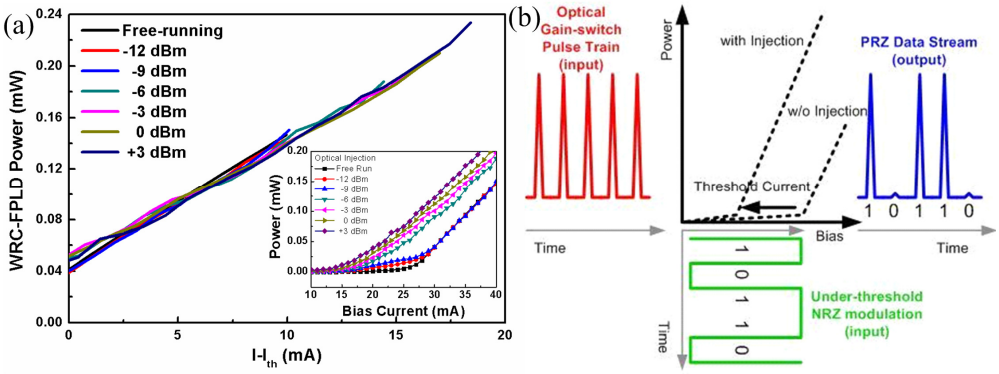

Fig. 2. (a) The power-current curve of the slave WRC-FPLD injection-locked by the master WRC-FPLD at different power levels. (b) The principle of the PRBS directly encoded slave WRC-FPLD RZ transmitter triggered by externally pulsated master WRC-FPLD injection.

Under external injection, the delivery of a pulsed RZ on-off-keying data stream from a slave WRC-FPLD requires the “on” bit current level of an NRZ modulation to be set slightly below the threshold current of the WRC-FPLD at a free-running condition, and a DC bias is added to offset the NRZ modulation data at half the threshold. In this case, the slave WRC-FPLD is un-lasing without the coherent injection by the master WRC-FPLD pulse-train, and the threshold reduction of the slave WRC-FPLD is adjusted by tuning the injection power level of the master WRC-FPLD pulse. This switches the operation of the slave WRC-FPLD between spontaneous emission and RZ data transmission. The slave WRC-FPLD is modulated directly at 2.5 Gbit/s to deliver a pulsed RZ data stream after it is coherently injection-locked by the DWDM-channelized master WRC-FPLD pulse-train. The master WRC-FPLD exhibits

#163683 - $15.00 USD Received 1 Mar 2012; revised 9 May 2012; accepted 12 May 2012; published 4 Jun 2012

the same device geometry as the slave, such that single-mode injection-locking is achieved without a detuning temperature for mode matching. The slave WRC-FPLD temporally blue-shifts its mode spectrum, whereas the master WRC-FPLD red-shifts its peak wavelength when the transient bias (because of the "on" bit current of the NRZ data) enlarges to a maximum. Hence, an enlarged tolerance on the mode wavelength deviation occurs between master and slave WRC-FPLDs. In the time domain, the gain-switched master WRC-FPLD pulsewidth can be optimized to 49 ps by setting the RF power up to + 8 dBm (Fig. 3). The relatively broadened pulsewidth is attributed to the longer cavity length of the WRC-FPLD, which inevitably lengthens the photon lifetime to degrade the gain-switching response limited by the square root of the product of photon and carrier lifetimes. Consequently, the master WRC-FPLD pulse has a substantially broadened longitudinal mode after gain-switching to increase the tolerance of the injection-locking wavelength. Figure 3 shows that the spectral linewidth of the master WRC-FPLD can be broadened from 0.2 (free-running) to 0.8 nm (with maximal RF power), which covers the entire AWG-channelized spectral window prior to the slave WRC-FPLD to be injection-locked. Because of the ultra-low front facet reflectance induced broadband gain spectrum of the WRC-FPLD, only one gain-switched master WRC-FPLD is used as the seeding source for injection-locking the WRC-FPLD transmitters at both down-stream (1510-1535 nm) and up-stream (1535-1560 nm) channels. The modes ranged between wavelength of 1510 and 1535 nm is used for injection-locking the down-stream WRC-FPLD transmitters, whereas the modes ranged between wavelength of 1535 and 1560 nm is used for injection-locking the up-stream WRC-FPLD transmitters.

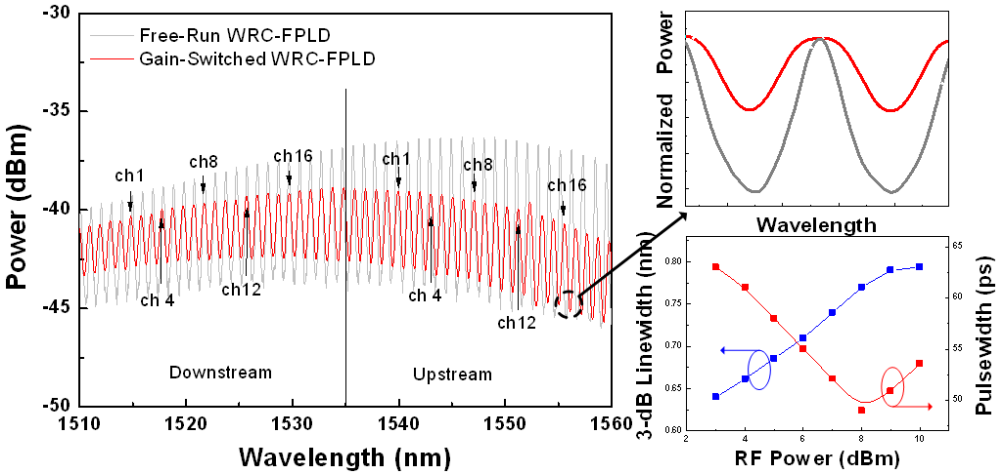

Fig. 3. Left: the optical spectra of the master WRC-FPLD operated at free-running (gray) and gain-switching (red) condition. Upper right: the normalized mode spectra at free-running (gray) and gain-switching (red) conditions. Lower right: the linewidth and pulsewidth of the master WRC-FPLD with different RF modulation powers.

Such a pulsated master WRC-FPLD pulse train with substantially broadened linewidth facilitates the injection-locking of the slave WRC-FPLD from a wider locking range, in which the side-mode suppression ratio (SMSR) and the on/off extinction ratio (ER) of the injection-locked WRC-FPLD can be optimized by detuning the optical injection power of the master WRC-FPLD. The peak power of the gain-switched pulse can be optimized without deforming the pulse shape by accurately controlling the microwave modulating power of the master WRC-FPLD. As shown in Fig. 4(a), the relatively broadened injection-locked wavelength range of the WRC-FPLD with an acceptable SMSR (>28 dB) is achieved, even when the injecting wavelength of the master WRC-FPLD pulse is detuned away from the longitudinal mode of the slave WRC-FPLD by ± 0.6 nm at a relatively high injection level (>0 dBm). Under a lower injection level, the injection-locking range of the slave WRC-FPLD shrinks

#163683 - $15.00 USD Received 1 Mar 2012; revised 9 May 2012; accepted 12 May 2012; published 4 Jun 2012

slightly to ± 0.4 nm for each longitudinal mode; however, it is 6–8 times larger than that of a standard FPLD. Both the injection-locking power and the end-face reflectance of the WRC-FPLD equally contribute to achieving the requested injection-locking wavelength range. Either a higher injection or a lower facet reflectance can promote broadband injection-locking. In the continuous-wave injection case, the unique low end-face reflectance feature of the WRC-FPLD effectively negates the requirement for high-level injection to cause a large wavelength shift of the slave WRC-FPLD during injection-locking. When using the pulsated WRC-FPLD master with a transient wavelength self-scanning function, the master WRC-FPLD mode with a wavelength swing can fulfill the spectral window of each AWG sliced DWDM channel. The transiently self-scanned master wavelength induces a wavelength tracking phenomenon during the injection locking process; therefore, the considerably broadened linewidth essentially benefits the easier injection-locking of the slave WRC-FPLD from an inferior wavelength mismatching condition. Consequently, such a wide injection-locking range negates the necessity for any self-feedback restorable wavelength locker set for the commercial FPLD-based upstream transmitter. The injection-locking power dependent wavelength lock-in range and the corresponding BER of the injection-locked WRC-FPLD transmitter shows in Fig. 4(b), which exhibits a broadened injection-locking wavelength range with an acceptable BER below 10^{-9}. In addition, the accepted injection-locking wavelength range for the 10^{-9} BER is proportional to the injection power.

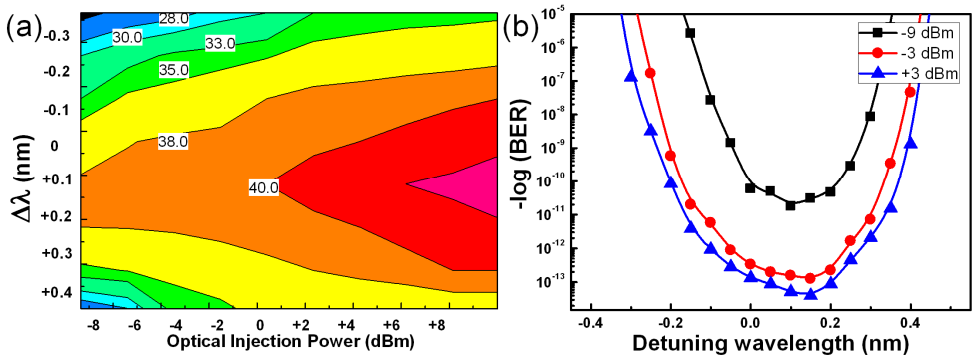

Fig. 4. The injection-locking power dependent wavelength lock-in range and the corresponding (a) SMSR and (b) BER of the slave WRC-FPLD transmitter.

After gain switching, the master WRC-FPLD broadens its longitudinal mode from 0.2 nm to 0.8 nm, as shown in Figs. 5 (a) and 6(b). In comparison with the spectrum-sliced ASE, such a 0.8-nm injection source provides a highly coherent injection into the slave WRC-FPLD with relatively lower intensity noise because of the highly attenuated spontaneous emission. With a sufficiently high coherence, the injection-locked WRC-FPLD can transmit up-stream data over a longer distance with a lower power budget. Under injection-locking with the master gain-switched WRC-FPLD, the linewidths of free-running and NRZ-modulating slave WRC-FPLD also broaden to 0.65 nm and 0.8 nm, as shown in Figs. 6(c) and 6(d).

#163683 - $15.00 USD Received 1 Mar 2012; revised 9 May 2012; accepted 12 May 2012; published 4 Jun 2012

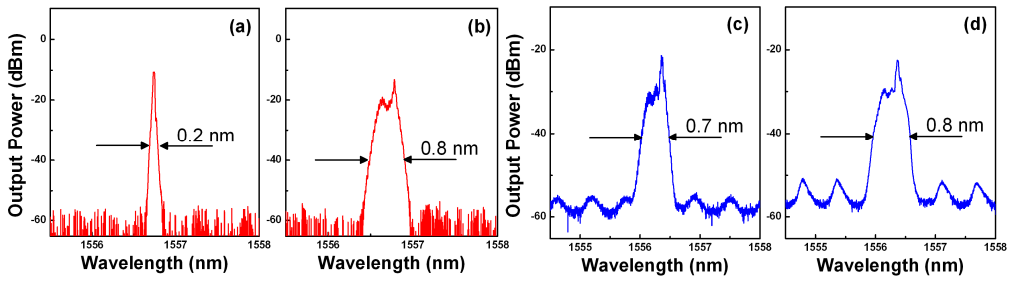

Fig. 5. (a) Free-running AWG sliced WRC-FPLD. (b) Gain-switched AWG sliced WRC-FPLD. (c) Free-running slave WRC-FPLD injected by gain-switched WRC-FPLD. (d) NRZ modulated slave WRC-FPLD injected by gain-switched WRC-FPLD.

The narrowing linewidth of the slave WRC-FPLD after injection-locking is caused by the spectral constraint of the slave WRC-FPLD longitudinal mode, which filters out the wavelength component from the injected master WRC-FPLD. The injection-induced dynamic threshold reduction linearly amplifies the modulated slave WRC-FPLD with a spectral linewidth controlled by the correlation of the master and slave longitudinal modes. Because the pulsated master WRC-FPLD provides a larger injection-locking bandwidth than commercial FPLDs, wavelength matching can be effectively optimized without the requirement of temperature control for the slave WRC-FPLD. The below-threshold modulation not only releases the temperature and the wavelength control of the slave WRC-FPLD, but also leads to the all-optical NRZ-to-RZ conversion under the optical carrier injection from the pulsed master source. Under the injection-locking condition, the stationary solution of the injection-locked slave WRC-FPLD must be re-derived using tracking rate equations [13,15],

$$\frac{dS(t)}{dt} = \frac{1}{2}\left[g(N(t)-N_{tr}) - \gamma_p \right] S(t) + \kappa\sqrt{S_{inj}(t)S(t)}\cos(\phi(t)), \tag{2}$$

$$\frac{d\phi(t)}{dt} = \frac{\alpha}{2}\left[g(N(t)-N_{tr}) - \gamma_p \right] - \kappa\sqrt{\frac{S_{inj}(t)}{S(t)}}\sin\phi(t) - \Delta\omega_{inj}, \tag{3}$$

$$\frac{dN(t)}{dt} = I(t) - \gamma_n N(t) - g[N(t)-N_{tr}]S(t), \tag{4}$$

where $S(t)$ denotes the photon number in the injection-locked mode, $N(t)$ the carrier number, N_{tr} the transparency carrier number, γ_p the photo decay rate, I the current, γ_n the carrier recombination rate, $\Delta\omega_{inj}$ the detuning frequency, $\phi(t)$ the phase, as expressed by $\phi(t) = \psi(t) - \psi_{inj}$, where $\psi(t)$ and ψ_{inj} are the difference between internal and injected fields and the phase of the injection WRC-FPLD respectively. Under coherent injection-locking, the internal field of the slave WRC-FPLD is changed by the master WRC-FPLD output to deviate the mode wavelength of the slave WRC-FPLD from the free-running condition. Before injection-locking, the wavelength of the slave WRC-FPLD is dynamically pulled toward one specific mode wavelength of the master WRC-FPLD after AWG-based DWDM channelization. Once the wavelength of the master WRC-FPLD changes, the wavelength of the slave WRC-FPLD tracks until injection-locking is stabilized. The shift between the master- and slave-mode wavelengths is a function of the injecting power and phase by solving the rate equations at a steady-state condition, as derived by

$$\Delta\omega_{inj} = -\kappa\sqrt{1+\alpha^2}\sqrt{\frac{S_{inj}}{S_0}}\sin\left(\tan^{-1}\alpha + \phi\right), \tag{5}$$

#163683 - $15.00 USD Received 1 Mar 2012; revised 9 May 2012; accepted 12 May 2012; published 4 Jun 2012

The detuning frequency ($\Delta\omega_{inj}$) is usually defined as the difference between the master frequency (ω_{ML}) and the free-running slave laser frequency (ω_{fr}). The detuning frequency can be enhanced by enlarging the injecting photon number, which is relatively easy to achieve because of the low end-face reflectance of the slave WRC-FPLD. To facilitate the modulating bandwidth, the proposed operating condition of the slave WRC-FPLD is DC biased at slightly below the threshold. With an enlarging power ratio of S_{inj}/S_0, the locking bandwidth of the quasi-color-free DWDM-PON can be substantially enhanced by a factor of 1.5-2.

To evaluate the dynamical variation of the mode spectral linewidth in the injection-locked slave WRC-FPLD under the master WRC-FPLD pulse seeding, the photon number of the master gain-switched WRC-FPLD injection can be simply assumed as a Gaussian function of $S_{inj} = S_i\exp(-t^2/\tau_0^2)$. Because of the spectral red-shift of the slave WRC-FPLD during gain switching induced by the transient variations of carrier concentration and the refraction index, the transient wavelength can be defined as $\lambda(t) = [n(t)*\lambda_0]/n_0$ with $n(t)$ and n_0 denoting as the transient and continuous-wave refractive indices of the WRC-FPLD, respectively. Assuming that the phase difference between the injected master and the injection-locked slave waves is adjusted to be completely in phase with $\cos\phi(t)\cong 1$), the wavelength shift during the gain-switched condition can be written as [16].

$$\begin{aligned}\Delta\lambda_{shift}(t) &= \lambda_{free-run} - \lambda_{gain-switching}(t) = \frac{\lambda_0}{n_0}\frac{dn}{dN}\left[N(t) - N_{th}\right] = \frac{\lambda_0}{n_0}\frac{dn}{dN}\frac{\tau_c}{qV}\left[I(t) - I'_{th,inj}\right] \\ &= \frac{\lambda_0}{n_0}\frac{dn}{dN}\frac{\tau_c}{qV}\left[I(t) - I_{th} + \frac{qV}{\tau_c}\left(\frac{2\kappa}{g}\frac{1}{\sqrt{1+\alpha^2}}\sqrt{\frac{S_i}{S_o}}e^{-\frac{t}{\tau_0}}\right)\right],\end{aligned} \tag{6}$$

where λ_0 is the wavelength of the free-running WRC-FPLD, and V is the active layer volume. Thus, the mean frequency deviation of the slave WRC-FPLD under the externally pulsed injection-locking condition can also be derived to yield a modal linewidth, which is written as

$$\begin{aligned}\Delta\lambda_{linewidth}(t) &= \frac{\lambda_0^2}{C}\Delta\nu_{linewidth}(t) = \frac{\lambda_0^2}{C}\frac{v_g\alpha_m h\nu R_{sp}}{4\pi P_{slave,out}(t)}(\alpha^2+1) \\ &= \frac{\lambda_0^2}{C}\frac{v_g\alpha_m h\nu R_{sp}(\alpha^2+1)}{4\pi}\left\{\frac{\eta_i h\nu\alpha_{eff}}{\tau_c}\left[N(t) - N_{th} + \left(\frac{2\kappa}{g}\frac{1}{\sqrt{1+\alpha^2}}\sqrt{\frac{S_i}{S_o}}e^{-\frac{t^2}{\tau_o^2}}\right)\right]\right\}^{-1} \\ &= \frac{\lambda_0^2}{C}\frac{v_g\alpha_m R_{sp}(\alpha^2+1)\tau_c}{4\pi\eta_i\alpha_{eff}}\left[N(t) - N_{th} + \left(\frac{2\kappa}{g}\frac{1}{\sqrt{1+\alpha^2}}\sqrt{\frac{S_i}{S_o}}e^{-\frac{t^2}{\tau_o^2}}\right)\right]^{-1} \\ &= \frac{\lambda_0^2}{C}\frac{v_g\alpha_m R_{sp}(\alpha^2+1)\tau_c}{4\pi\eta_i\alpha_{eff}}\left[\frac{\tau_c}{q}\left[I(t) - I_{th}\right] + \left(\frac{2\kappa}{g}\frac{1}{\sqrt{1+\alpha^2}}\sqrt{\frac{S_i}{S_o}}e^{-\frac{t^2}{\tau_o^2}}\right)\right]^{-1},\end{aligned} \tag{7}$$

where C denotes speed of light, R_{sp} the spontaneous emission rate, η_i the internal quantum efficiency, $h\nu$ the energy per photon, $\alpha_{eff} = [\alpha_m/(\langle\alpha_i\rangle + \alpha_m)]$ the effective loss factor, α_m the facet loss, and $\langle\alpha_i\rangle$ the internal loss. In a general case with continuous-wave lasing or small-signal modulation, the output power of the WRC-FPLD does not vary substantially to affect the spectral distribution. Under gain-switched pulsation, the total wavelength scanning range,

#163683 - $15.00 USD Received 1 Mar 2012; revised 9 May 2012; accepted 12 May 2012; published 4 Jun 2012

$\Delta\lambda_{total}(t)$, of the transient injection-locked slave WRC-FPLD is the summation of the transient wavelength shift ($\Delta\lambda_{shift}$) and transient linewidth broadening ($\Delta\lambda_{linewidth}$), as derived by

$$\Delta\lambda_{total}(t)=\frac{\frac{\lambda_0}{n_0}\frac{dn}{dN}\frac{\tau_c^2}{q^2V}\left[I(t)-I_{th}+\frac{qV}{\tau_c}\left(\frac{2\kappa}{g}\frac{1}{\sqrt{1+\alpha^2}}\sqrt{\frac{S_i}{S_o}}e^{-\frac{t^2}{\tau_0^2}}\right)\right]^2+\frac{\lambda_0^2}{C}\frac{v_g\alpha_m R_{sp}(\alpha^2+1)\tau_c}{4\pi\eta_i\alpha_{eff}}}{\frac{\tau_c}{q}\left[I(t)-I_{th}+\frac{qV}{\tau_c}\left(\frac{2\kappa}{g}\frac{1}{\sqrt{1+\alpha^2}}\sqrt{\frac{S_i}{S_o}}e^{-\frac{t^2}{\tau_0^2}}\right)\right]}, \tag{8}$$

When operating, the slave WRC-FPLD is slightly biased below the threshold. To realize the dynamical linewidth of the master laser source, we assumed that the master laser is nonlinearly modulated by an amplified sinusoidal wave, and that the DC-biased point is slightly offset away from the threshold to provide the gain-switching output power of

$$P_{out}(t)=\eta_i\alpha_{eff}[I(t)-I_{th}]=\eta_i\alpha_{eff}\Delta I\sin(2\pi f_m t), \tag{9}$$

where ΔI denotes the amplitude-modulated current of the sinusoidal RF signal, and f_m denotes the modulation frequency. With a modulation current simplified as $I(t)$-I_{th} = $\Delta I[\sin(2\pi f_m t)]$, the total wavelength scanning range of the slave WRC-FPLD under direct modulation and pulsed optical injection is derived by

$$\Delta\lambda_{total}(t)\cong\frac{\frac{\lambda_0}{n_0}\frac{dn}{dN}\frac{\tau_c^2}{q^2V}\left[\Delta I\sin(2\pi f_m t)+\frac{qV}{\tau_c}\left(\frac{2\kappa}{g}\frac{1}{\sqrt{1+\alpha^2}}\sqrt{\frac{S_i}{S_o}}e^{-\frac{t^2}{\tau_0^2}}\right)\right]^2+\frac{\lambda_0^2}{C}\frac{v_g\alpha_m R_{sp}(\alpha^2+1)\tau_c}{4\pi\eta_i\alpha_{eff}}}{\frac{\tau_c}{q}\left[\Delta I\sin(2\pi f_m t)+\frac{qV}{\tau_c}\left(\frac{2\kappa}{g}\frac{1}{\sqrt{1+\alpha^2}}\sqrt{\frac{S_i}{S_o}}e^{-\frac{t^2}{\tau_0^2}}\right)\right]}, \tag{10}$$

The parameters of the WRC-FPLD used for all simulations in this study are listed in Table 1.

Table 1. Injection-locked WRC-FPLD parameters

Parameters	Symbol	Value	Units
Internal quantum efficiency	η_i	0.8	
Electron charge	Q	1.6×10^{-19}	C
Spontaneous carrier lifetime	τ_c	2.71×10^{-9}	s
Velocity	v_g	0.857×10^{8}	m/s
Differential gain	A	5.34×10^{-20}	m^2
Active region length	L	600×10^{-6}	m
Active region width	W	15×10^{-6}	m
Active region thickness	D	0.081×10^{-6}	m
Transparency carrier number	N_{tr}	29.2×10^{7}	
Linewidth enhancement factor	α	3	
Optical confinement factor	Γ	0.23	
Photon lifetime	τ_p	1.4244×10^{-12}	s
Coupling rate	κ	7.1065×10^{11}	s^{-1}
Spontaneous emission rate	R_{sp}	2×10^{12}	s^{-1}
Stimulated emission rate	g	6.28×10^{3}	s^{-1}

When injection-locking by a transient wavelength scanning pulse from the master WRC-FPLD, the simulated linewidth of the slave WRC-FPLD mode also shows a broadening effect because of the pulsed injection-induced threshold reduction and gain-switching, as displayed

#163683 - $15.00 USD Received 1 Mar 2012; revised 9 May 2012; accepted 12 May 2012; published 4 Jun 2012

in Fig. 6. As shown in Eq. (6), the linewidth of the gain-switching slave WRC-FPLD in this study is simultaneously proportional to the modulation current and the injection power. Under external injection, the threshold current of the slave WRC-FPLD is slightly reduced, which leads the WRC-FPLD from spontaneous emission to a gain-switching operation; therefore, the effective modulation current of the injection-locked slave WRC-FPLD is influenced by the injection power of the master WRC-FPLD. Consequently, the simulation shows that the linewidth of the slave WRC-FPLD is also reduced because of the injection-locking-induced coherence enhancement, as shown in Eq. (7). In summary, such an operation leads to an increased modulation current by enlarging the injection power, which concurrently causes linewidth narrowing and transient shifting effects on the longitudinal mode. Based on these simulations, transient wavelength shifting plays a vital role in dynamic linewidth broadening. The longitudinal mode is switched quickly by the pulsed master, and switching speed is accelerated by the photon lifetime of the slave WRC-FPLD. The right subfigure in Fig. 6 shows the net wavelength shift and linewidth of one injection-locked longitudinal mode in the slave WRC-FPLD under injection-locking by the pulsed master WRC-FPLD at different injection powers. Because of the transient wavelength self-scanning and self-tracked injection-locking by the master WRC-FPLD pulse, the net wavelength shift is increased and the injection-locked linewidth is narrowed for the slave WRC-FPLD. When injection-locking by a transient wavelength scanning pulse from the master WRC-FPLD, the weight of the transient wavelength shift is higher than the linewidth broadening of the injection-locked slave WRC-FPLD. That is, the injection-locked spectrum of the slave WRC-FPLD is actually not broadened but transiently shifted by the pulsed master WRC-FPLD.

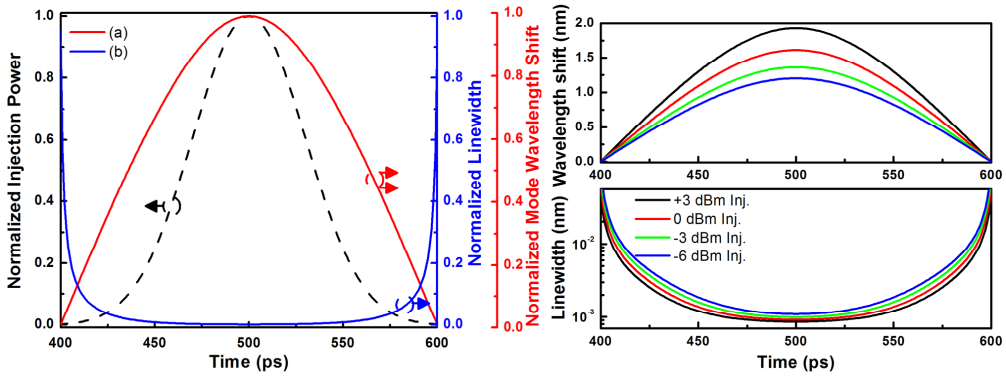

Fig. 6. Left: the simulated change of the linewidth and wavelength shift for the slave WRC-FPLD as a function of the delay time and the injection power of the master WRC-FPLD injection with Gaussian profile. Right: the net wavelength shift and linewidth of one injection-locked longitudinal mode in the slave WRC-FPLD under the injection of the pulsed master WRC-FPLD injection at different powers.

One characteristic feature of such an injection-locked slave WRC-FPLD is its spectral invariance during temperature fluctuation. Because the coherent injection-locking of the slave WRC-FPLD is initiated from the spontaneous emission regime, its wavelength spectrum is completely controlled by the externally injected master WRC-FPLD pulse. Even the wavelength of the free-running WRC-FPLD is drifted with device temperature; such a wavelength drift is eliminated by the coherent injection because the coherent master source pins the slave source at its modal wavelength. In the free-running case, the mode spectrum of the slave WRC-FPLD persistently shifts within the 200-GHz AWG DWDM channel to change its mode numbers between 2 and 3 within each channel, and the AWG-filtered mode numbers decrease as the temperature increases to 29°C. However, the transient coherent injection from the master WRC-FPLD introduces a dynamic red-shift on the longitudinal mode wavelength, such that the longitudinal mode of the slave WRC-FPLD is pushed to

#163683 - $15.00 USD Received 1 Mar 2012; revised 9 May 2012; accepted 12 May 2012; published 4 Jun 2012

injection-lock with the broadened mode delivered from the pulsed master, as shown in Fig. 7. By contrast, the ASE injection-locking technique fails to control the injection-locked mode number of the slave WRC-FPLD within one AWG channel because the ultra-wideband ASE spectrum allows the slave WRC-FPLD to arbitrarily shift its mode and be injection-locked at any case. In comparison with the proposed injection-locking scheme with a pulsed coherent master, the required power budget of a non-coherent ASE master per optical-network-unit (ONU) channel is difficult to achieve because the non-coherent CW injection level is substantially larger than that of the pulsed coherent master. That is, the gain-switched operation of the master WRC-FPLD can deliver a higher peak power after linking with the same EDFA to improve the wavelength injection-locking range and the injection-locked mode linewidth by using the coherent pulsed injection without sacrificing the power budget per channel.

To evaluate the temperature influence of the WRC-FPLD, the injection-locked slave WRC-FPLD output spectra are measured at temperatures ranging from 21°C to 29°C. The temperature-dependent wavelength red-shift for the free-running slave WRC-FPLD is determined as 0.08 nm/°C. Within the detuning temperature range, the injection-locked slave WRC-FPLD spectrum is stable and invariant, with the original wavelength deviation between the master and slave WRC-FPLDs, as shown in Fig. 8(a). Because wavelength shifting is induced by changing the inner photon density of the WRC-FPLD, the efficiency of the optical injection is strongly affected by the Fabry-Perot etalon effect in WRC-FPLDs. The over-power injection-induced shifting is counteracted by the lower injection efficiency to maintain wavelength stability. Such a pulsated master injection-locked slave WRC-FPLD behaves similarly to a dynamic wavelength sweeper, which induces mode injection-locking between the master and slave WRC-FPLDs. The wavelength-selection can be ignored in such a quasi-color-free WRC-FPLD because the maximal wavelength sweeping range of the pulsed master WRC-FPLD is wider than the injection-locking range of the slave WRC-FPLD.

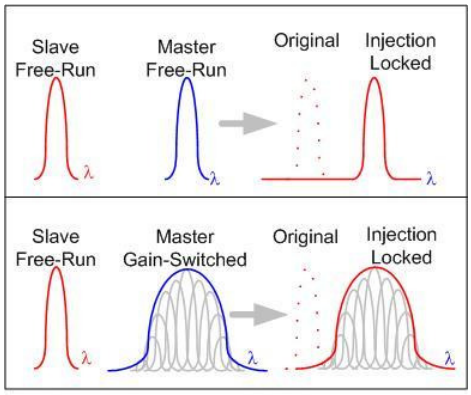

Fig. 7. The schematic diagram of single-wavelength injection and gain-switched injection.

#163683 - $15.00 USD Received 1 Mar 2012; revised 9 May 2012; accepted 12 May 2012; published 4 Jun 2012

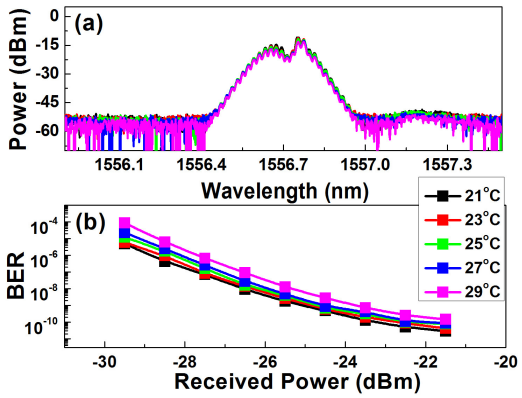

Fig. 8. (a) The optical spectrum and (b) the BER of injected WRC-FPLD at temperature from 21°C to 29°C.

As shown in Fig. 8(b), only a small positive power penalty occurred on BER by 0.6 dB during the sweep of the slave WRC-FPLD temperature. That is, only power attenuation occurs during the temperature change of the slave WRC-FPLD, leading to a degradation of the inner lasing efficiency, which is more pronounced than the wavelength matching effect. Consequently, the receiving power at a specific BER must be enlarged inevitably by increasing the WRC-FPLD operating temperature. However, such a degradation induces a power penalty of less than 1 dB within 21-29°C. Finally, the quasi-color-free RZ transmission by the pulsated master WRC-FPLD injection-locked slave WRC-FPLD can be achieved in up to 16 DWDM channels. The transmitted RZ data stream is all-optical converted from the modulated NRZ data stream, and the measured BER transmission performance for up- and down-stream transmission versus receiving power is shown in Fig. 9. A receiving sensitivity of −26.6 dBm can be achieved for 2.5 Gbit/s back-to-back up-stream transmission at BER<10^{-10}. A well-opened RZ eye pattern with acceptable intensity noise is obtained with a relatively large dynamic range, in which the rising and falling times are 48 and 52 ps, respectively. The highest and lowest power penalties of the adjacent 16 channels for up-stream transmission after 25-km SMF propagation are 0.9 dB and 2 dB, respectively. The increasing power penalty for side-mode injection-locked WRC-FPLDs is affected by the intrinsic difference among their mode powers and the linear-dispersion data transmission distortion. With appropriate temperature tuning on each slave WRC-FPLD, the variation on receiver sensitivity penalty at BER = 10^{-10} can be confined within 1.6 dB under a temperature shift below 15°C. The acceptable tolerance on the wavelength-locking bandwidth can be enhanced by increasing RF power to further broaden gain-switching modal linewidth. Because the up- and down-stream WRC-FPLD slave transmitters are injection-locked by the same pulsed master WRC-FPLD seeding source, the spectral intensity profile of the modes distributed between 1510 and 1565 nm are relatively flattened with a peak intensity of only $\Delta P/\Delta\lambda$<0.08 dB/nm. This trivial deviation also preserves the similarity of each DWDM-PON channel on the injection-locking power budget. As a result, all of the up- and down-stream WRC-FPLD slave transmitters request almost identical injection-locking power level from the seeding master WRC-FPLD source. With a constant injection-locking power, the down- and up-stream WRC-FPLD slave transmitters reveal roughly the same BER transmission performance with a receiving power sensitivity deviation of only 1.1 dB and 1.3 dB, respectively. The slight difference between the power penalties of the down- and up-stream transmission channels is caused by the degradation of SNR and ER for the pulsed WRC-FPLD master propagating along the DWDM-PON with a distance of 25 km. By adjusting the cavity length, the longitudinal mode spacing of the master WRC-FPLD can be modified to match the ITU-T-defined DWDM channels for practical DWDM-PON applications.

#163683 - $15.00 USD Received 1 Mar 2012; revised 9 May 2012; accepted 12 May 2012; published 4 Jun 2012

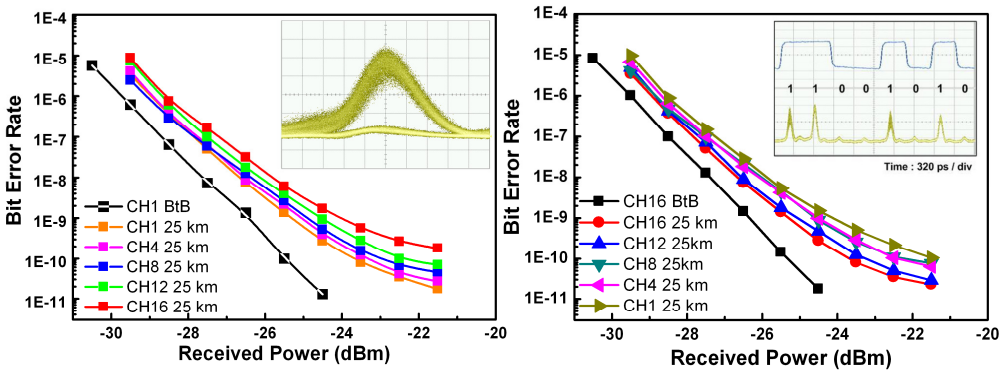

Fig. 9. BER analysis of wavelength injection locked WRC-FPLD at different channels for up- (left) and down-stream (right) transmission, and the measured pulsed RZ eye diagrams (inset).

5. Conclusion

With the transient wavelength scanning and tracking, both the down- and up-stream slave WRC-FPLDs are directly modulated by PRBS NRZ data and coherently injection-locked by the master gain-switched WRC-FPLD after 200-GHz AWG channelization to perform the bi-directional RZ data transmission at 2.5 Gbit/s over 25 km. The proposed scheme uses a gain-switched WRC-FPLD as a coherent injection source with lower noise than an ASE source, and the quasi-color-free WRC-FPLD transmitters with relatively larger tolerance on injection-locking bandwidth. This study performs numerical simulations of the transient wavelength shifting and the linewidth broadening for the slave WRC-FPLD during the injection-locking induced gain-switching operation, which helps to optimize the injection-locking range of the slave WRC-FPLD for delivering the RZ data stream with a bit rate of up to 2.5 Gbit/s. Even if the wavelength of the free-running WRC-FPLD is drifted with device temperature, such a wavelength drift is eliminated by the injection locking because the coherent master source pins the slave source at its modal wavelength. By tuning the temperature of the slave WRC-FPLD between 21°C and 29°C, the BER degrades with a power penalty of only < 1dB. Back-to-back receiving sensitivities with best and worst transmission performance are −25.6 and −23.6 dBm, respectively, and the rising and the falling time of the pulsed RZ eye pattern is obtained with 48 and 52 ps. The optimal side-mode suppression ratio of 42 dB and the lowest timing root-mean-square jitter of 16 ps for the pulsed RZ data stream are also observed. This system is a balance between coherent and incoherent injection. The identical master and slave WRC-FPLDs at central office and optical network unit essentially provide the quasi-color-free DWDM-PON universal transmitters with broadband wavelength tunability and suppressed noise figure when compared with RSOAs. The pulsed RZ data stream can be applied to the RZ binary-phase-shift-keying (BPSK) network or the hybrid DWDM/OTDM PON architecture.

Acknowledgments

The authors thank the National Science Council of Republic of China and the Chunghwa Telecom Co., Ltd. for financially supporting this research under grants NSC98-2221-E-002-023-MY3, NSC100-2221-E-002-156-MY3, and 100-SC-23, respectively.

#163683 - $15.00 USD Received 1 Mar 2012; revised 9 May 2012; accepted 12 May 2012; published 4 Jun 2012